Fault-Tolerant Control of a Polyethylene Reactor

Adiwinata Gani, Prashant Mhaskar[†] and Panagiotis D. Christofides[‡]
Department of Chemical and Biomolecular Engineering
University of California, Los Angeles, CA 90095

***Abstract*— This work focuses on fault-tolerant nonlinear control of a gas phase polyethylene reactor. Initially, a family of candidate control configurations, characterized by different manipulated inputs, are identified. For each control configuration, a bounded nonlinear feedback controller, that enforces asymptotic closed-loop stability in the presence of constraints, is designed, and the constrained stability region associated with it is explicitly characterized using Lyapunov-based tools. A switching policy is then derived, on the basis of the stability regions, to orchestrate the activation/deactivation of the constituent control configurations in a way that guarantees closed-loop stability in the event of control system faults. Closed-loop system simulations demonstrate the effectiveness of the fault-tolerant control strategy.**

I. Introduction

Increasingly faced with the requirements of safety, reliability, and profitability, chemical process operation is relying extensively on highly automated process control systems. Automation, however, tends to increase vulnerability of the process to faults (for example, defects/malfunctions in process equipment, sensors and actuators, faults in the controllers or in the control loops) potentially causing a host of economic, environmental, and safety problems that can seriously degrade the operating efficiency of the process. Problems due to faults may include physical damage to the process equipment, increase in the wasteful use of raw material and energy resources, increase in the downtime for process operation resulting in significant production losses, and jeopardizing personnel and environmental safety. These considerations provide a strong motivation for the development of methods for the design of advanced fault-tolerant control systems that ensure an efficient and timely response to enhance fault recovery and prevent faults from propagating or developing into total faults.

Fault-tolerant control has been an active area of research for the past ten years, and has motivated many research studies in this area within the context of aerospace engineering (see, for example, [18], [3], [24]). The whole notion of fault-tolerant control is based on the underlying assumption of the availability of more control configurations than required. Under this assumption, the reliable control approach dictates use of all the control loops at the same time so that fault of one control loop does not lead to the fault of the entire control structure (for example, [23], [20]). The use of only as many control loops as are required at a time, is often motivated by economic considerations (to save on unnecessary control action), and in this case, fault-tolerant control can be achieved through control-loop reconfiguration. Recently, fault-tolerant control has gained increased attention within process control; however, the available results have been based on the assumption of a linear process description [13], [21], [1], [19].

Switching to fall-back control configurations in the event of faults results in an overall process that exhibits intervals of piecewise continuous behavior interspersed by discrete transitions. A hybrid systems framework therefore provides a natural setting for the analysis and design of fault-tolerant control structures. However, at this stage, despite the large and growing body of research work on a diverse array of hybrid system problems (e.g., [12], [11], [6], [2], [9]), the use of a hybrid system framework for the study of fault-tolerant control problems has received limited attention. In [10], a hybrid systems approach to fault-tolerant control was employed where upon occurrence of a fault, stability region-based reconfiguration is done to achieve fault-tolerant control. In [17], the problem of implementing integrated fault-detection and fault-tolerant control was addressed under state and output feedback. Designing fault-tolerant control structures that prevent loss of product (due to limit cycles) and possible loss of equipment (due to unacceptably high temperatures) in the event of a fault in the control configuration is therefore of important industrial value.

This work focuses on fault-tolerant control of a gas phase polyethylene reactor modeled by seven nonlinear ODEs. Polyethylene is the most popular of all synthetic commodity polymers, with current worldwide production of more than 40 billion tonnes per year. Large proportion of this polyethylene is produced in gas phase reactors using Ziegler-Natta catalysts. In gas phase polyethylene reactor, the temperature in the reaction zone is kept above the dew point of the reactant and below the melting point of the polymer to prevent melting and consequent agglomeration of the product particles. Most commercial gas phase fluidized bed polyethylene reactors are operated in a relatively narrow temperature range between $75^{\circ}C$ and $110^{\circ}C$ [22]. It has been demonstrated [4], [16], [14] that without feedback temperature control, industrial gas phase polyethylene reactors are prone to unstable steady-states, limit cycles, and excursions toward unacceptable high temperature steady-states.

[†] Current address: Department of Chemical Engineering, McMaster University, Ontario, Canada
[‡] Corresponding author. Email: pdc@seas.ucla.edu
Financial support by NSF, CTS-0529295, is gratefully acknowledged.

To develop a fault-tolerant control system for a gas phase polyethylene reactor, we initially identify a family of candidate control configurations, characterized by different manipulated inputs on the basis of a detailed model of the process. For each control configuration, a bounded nonlinear feedback controller, that enforces asymptotic closed-loop stability in the presence of constraints, is designed, and the constrained stability region associated with it is explicitly characterized using Lyapunov-based tools. A switching policy is then derived, on the basis of the stability regions, to orchestrate the activation/deactivation of the constituent control configurations in a way that guarantees closed-loop stability in the event of control system faults. Closed-loop system simulations demonstrate the effectiveness of the fault-tolerant control strategy.

II. Process description and modeling

Figure 1 shows a schematic of an industrial gas phase polyethylene reactor system. The feed to the reactor consists of ethylene, comonomer, hydrogen, inerts, and catalyst. A stream of unreacted gases flows from the top of the reactor and is cooled by passing through a heat exchanger in counter-current flow with cooling water. Cooling rates in the heat exchanger are adjusted by instantaneously blending cold and warm water streams while maintaining a constant total cooling water flowrate through the heat exchanger. Mass balance on hydrogen and comonomer have not been considered in this study because hydrogen and comonomer have only mild effects on the reactor dynamics [16]. A mathematical model for this reactor has the form [5]:

$$\begin{aligned}
\frac{d[In]}{dt} &= \frac{F_{In} - \frac{[In]}{[M_1]+[In]} b_t}{V_g} \\
\frac{d[M_1]}{dt} &= \frac{F_{M_1} - \frac{[M_1]}{[M_1]+[In]} b_t - R_{M1}}{V_g} \\
\frac{dY_1}{dt} &= F_c a_c - k_{d_1} Y_1 - \frac{R_{M1} M_{W_1} Y_1}{B_w} \\
\frac{dY_2}{dt} &= F_c a_c - k_{d_2} Y_2 - \frac{R_{M1} M_{W_1} Y_2}{B_w} \\
\frac{dT}{dt} &= \frac{H_f + H_{g1} - H_{g0} - H_r - H_{pol}}{M_r C_{pr} + B_w C_{ppol}} \\
\frac{dT_{w_1}}{dt} &= \frac{F_w}{M_w}(T_{wi} - T_{w_1}) - \frac{UA}{M_w C_{pw}}(T_{w_1} - T_{g_1}) \\
\frac{dT_{g_1}}{dt} &= \frac{F_g}{M_g}(T - T_{g_1}) + \frac{UA}{M_g C_{pg}}(T_{w_1} - T_{g_1})
\end{aligned} \tag{1}$$

where

$$\begin{aligned}
b_t &= V_p C_v \sqrt{([M_1]+[In]) \cdot RR \cdot T - P_v} \\
R_{M1} &= [M_1] \cdot k_{p0} \cdot exp[\tfrac{-E_a}{R}(\tfrac{1}{T} - \tfrac{1}{T_f})] \cdot (Y_1 + Y_2) \\
C_{pg} &= \tfrac{[M_1]}{[M_1]+[In]} C_{pm1} + \tfrac{[In]}{[M_1]+[In]} C_{pIn} \\
H_f &= F_{M_1} C_{pm1}(T_{feed} - T_f) \\
&\quad + F_{In} C_{pIn}(T_{feed} - T_f) \\
H_{g1} &= F_g (T_{g_1} - T_f) C_{pg} \\
H_{g0} &= (F_g + b_t)(T - T_f) C_{pg} \\
H_r &= H_{reac} M_{W_1} R_{M1} \\
H_{pol} &= C_{ppol}(T - T_f) R_{M1} M_{W_1}
\end{aligned} \tag{2}$$

Table I includes the definition of all the variables used in Eqs.1-2.

TABLE I
PROCESS VARIABLES.

a_c	active site concentration of catalyst
b_t	overhead gas bleed
B_w	mass of polymer in the fluidized bed
C_{pm1}	specific heat capacity of ethylene
C_v	vent flow coefficient
C_{pw}	specific heat capacity of the water
C_{pIn}	specific heat capacity of the inert gas
C_{ppol}	specific heat capacity of the polymer
E_a	activation energy
F_c	flow rate of catalyst
F_g	flow rate of recycle gas
F_{In}	flow rate of inert
F_{M_1}	flow rate of ethylene
F_w	flow rate of cooling water
H_f	enthalpy of fresh feed stream
H_{g0}	enthalpy of total gas outflow stream from reactor
H_{g1}	enthalpy of cooled recycle gas stream to reactor
H_{pol}	enthalpy of polymer
H_r	heat liberated by polymerization reaction
H_{reac}	heat of reaction
$[In]$	molar concentration of inerts in the gas phase
k_{d_1}	deactivation rate constant for catalyst site 1
k_{d_2}	deactivation rate constant for catalyst site 2
k_{p0}	pre-exponential factor for polymer propagation rate
$[M_1]$	molar concentration of ethylene in the gas phase
M_g	mass holdup of gas stream in heat exchanger
$M_r C_{pr}$	product of mass and heat capacity of reactor walls
M_w	mass holdup of cooling water in heat exchanger
M_{W_1}	molecular weight of monomer
P_v	pressure downstream of bleed vent
R	ideal gas constant, unit of $\frac{J}{mol \cdot K}$
RR	ideal gas constant, unit of $\frac{m^3 \cdot atm}{mol \cdot K}$
T	reactor temperature
T_f	reference temperature
T_{feed}	feed temperature
T_{g_1}	temperature of recycle gas stream from exchanger
T_{w_1}	temperature of cooling water stream from exchanger
T_{wi}	inlet cooling water temperature to heat exchanger
UA	product of heat exchanger coefficient with area
V_g	volume of gas phase in the reactor
V_p	bleed stream valve position
Y_1	moles of active site type 1
Y_2	moles of active site type 2

The values of the process parameters are listed in Table II. It was verified that under these operating conditions, the

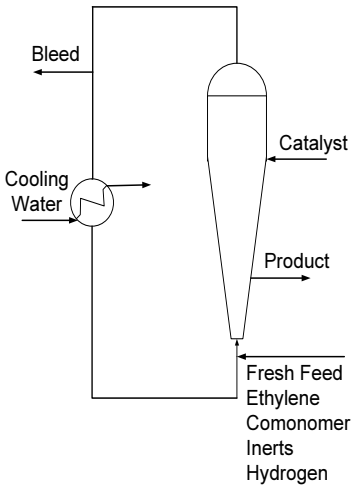

Fig. 1. Industrial gas phase polyethylene reactor system.

TABLE II

PARAMETER VALUES AND UNITS [5].

V_g	=	500	m^3
V_p	=	0.5	
P_v	=	17	atm
B_w	=	$7 \cdot 10^4$	kg
k_{p0}	=	$85 \cdot 10^{-3}$	$\frac{m^3}{mol \cdot s}$
E_a	=	$(9000)(4.1868)$	$\frac{J}{mol}$
C_{pm1}	=	$(11)(4.1868)$	$\frac{J}{mol \cdot K}$
C_v	=	7.5	$atm^{-0.5}\frac{mol}{s}$
C_{pw}	=	$(10^3)(4.1868)$	$\frac{J}{kg \cdot K}$
C_{pIn}	=	$(6.9)(4.1868)$	$\frac{J}{mol \cdot K}$
C_{ppol}	=	$(0.85 \cdot 10^3)(4.1868)$	$\frac{J}{kg \cdot K}$
k_{d_1}	=	0.0001	s^{-1}
k_{d_2}	=	0.0001	s^{-1}
M_{W_1}	=	$28.05 \cdot 10^{-3}$	$\frac{kg}{mol}$
M_w	=	$3.314 \cdot 10^4$	kg
M_g	=	6060.5	mol
$M_r C_{pr}$	=	$(1.4 \cdot 10^7)(4.1868)$	$\frac{J}{K}$
H_{reac}	=	$(-894 \cdot 10^3)(4.1868)$	$\frac{J}{kg}$
UA	=	$(1.14 \cdot 10^6)(4.1868)$	$\frac{J}{K \cdot s}$
F_{In}	=	5	$\frac{mol}{s}$
F_{M_1}	=	190	$\frac{mol}{s}$
F_g	=	8500	$\frac{mol}{s}$
F_w	=	$(3.11 \cdot 10^5)(18 \cdot 10^{-3})$	$\frac{kg}{s}$
F_c^s	=	$\frac{5.8}{3600}$	$\frac{kg}{s}$
T_f	=	360	K
T_{feed}^s	=	293	K
T_{wi}	=	289.56	K
RR	=	$8.20575 \cdot 10^{-5}$	$\frac{m^3 \cdot atm}{mol \cdot K}$
R	=	8.314	$\frac{J}{mol \cdot K}$
a_c	=	0.548	$\frac{mol}{kg}$
u_1^{max}	=	$5.78 \cdot 10^{-4}$	$\frac{K}{s}$
u_2^{max}	=	$3.04 \cdot 10^{-4}$	$\frac{mol}{s}$
$[In]_s$	=	439.68	$\frac{mol}{m^3}$
$[M_1]_s$	=	326.72	$\frac{mol}{m^3}$
Y_{1_s}	=	3.835	mol
Y_{2_s}	=	3.835	mol
T_s	=	356.21	K
$T_{w_{1_s}}$	=	290.37	K
$T_{g_{1_s}}$	=	294.36	K

open-loop system behaves in an oscillatory fashion (i.e., the system possesses an open-loop unstable steady-state surrounded by a limit cycle).

The control objective is to stabilize the reactor. To accomplish this objective in the presence of control system faults, we consider the following manipulated input candidates:

1) Feed temperature, $u_1 = \frac{F_{M_1}C_{pm1}+F_{In}C_{pIn}}{M_rC_{pr}+B_wC_{ppol}}(T_{feed} - T_{feed}^s)$, subject to the constraint $|u_1| \leq u_{max}^1 = \frac{F_{M_1}^s C_{pm1}+F_{In}C_{pIn}}{M_rC_{pr}+B_wC_{ppol}}(20)\ \frac{K}{s}$.
2) Catalyst flowrate, $u_2 = (F_c - F_c^s)a_c$, subject to the constraint $|u_2| \leq u_{max}^2 = (\frac{2}{3600})a_c\ \frac{mol}{s}$.

Each of the above manipulated inputs represents a unique control configuration (or control loop) that, by itself, can stabilize the reactor. The first control configuration, with feed temperature (T_{feed}) as the manipulated input, will be considered as the primary configuration. In the event of some faults in this configuration, however, the plant supervisor, will have to activate the fall-back configuration in order to maintain closed-loop stability. The question which we address in the next section, is how the supervisor determines if the fall-back control configuration will be able to stabilize the reactor if the primary control configuration fails.

III. FAULT-TOLERANT CONTROL

Having identified the candidate control configurations that can be used, we outline in this section the main steps involved in the fault-tolerant control system design procedure. These include: (1) the synthesis of a stabilizing feedback controller for each control configuration, (2) the explicit characterization of the constrained stability region associated with each configuration, and (3) the design of a switching law that orchestrates the re-configuration of control system in a way that guarantees closed-loop stability in the event of faults in the active control configuration.

To present our results in an compact form, we write the model of Eq.1 in a deviation (from the operating unstable steady-state) variable form, by defining $x = [x_1\ \ x_2\ \ x_3\ \ x_4\ \ x_5\ \ x_6\ \ x_7]^T$ where $x_1 = In - In_s$, $x_2 = M_1 - M_{1_s}$, $x_3 = Y_1 - Y_{1_s}$, $x_4 = Y_2 - Y_{2_s}$, $x_5 = T - T_s$, $x_6 = T_{w_1} - T_{w_{1_s}}$, $x_7 = T_{g_1} - T_{g_{1_s}}$, and obtain a continuous-time nonlinear system with the following state-space description:

$$\begin{array}{rcl} \dot{x}(t) & = & f_{k(t)}(x(t)) + g_{k(t)}(x(t))u_{k(t)} \\ |u_{k(t)}| & \leq & u_k^{max} \\ k(t) & \in & \mathcal{K} = \{1, 2\} \end{array} \quad (3)$$

where $x(t) \in \mathbb{R}^7$ denotes the vector of process state variables and $u_k(t) \in [-u_k^{max}, u_k^{max}] \subset \mathbb{R}$ denotes the constrained manipulated input associated with the k-th control configuration. $k(t)$, which takes values in the finite index set $\mathcal{K}$, represents a discrete state that indexes the vector fields $f_k(\cdot)$, $g_k(\cdot)$ as well as the manipulated input $u_k(\cdot)$. The explicit form of the vector fields $f_{k(t)}(x(t))$ and $g_{k(t)}(x(t))$ can be obtained by comparing Eq.1 and

Eq.3 and is omitted for brevity. For each value that k assumes in $\mathcal{K}$, the process is controlled via a different manipulated input which defines a given control configuration. Switching between the available two control configurations is controlled by a higher-level supervisor that monitors the process and orchestrates, accordingly, the transition between the different control configurations in the event of control system fault. This in turn determines the temporal evolution of the discrete state, $k(t)$. The supervisor ensures that only one control configuration is active at any given time, and allows only a finite number of switches over any finite interval of time. The control objective is to stabilize the process of Eq.3 in the presence of actuator constraints and faults in the control system. The basic problem is how to coordinate switching between the different control configurations (or manipulated inputs) in a way that respects actuator constraints and guarantees closed-loop stability in the event of faults. To simplify the presentation of our results, we will focus only on the state feedback problem where measurements of all process states are available for all times.

(a) *Constrained feedback controller synthesis:*

In this step, we synthesize, for each control configuration, a feedback controller that enforces asymptotic closed-loop stability in the presence of actuator constraints. This task is carried out on the basis of the process input/output dynamics. While our control objective is to achieve full state stabilization, process outputs are introduced only to facilitate transforming the system of Eq.1 into a form more suitable for explicit controller synthesis.

1. For the primary control configuration with $u_1 = \frac{F_{M_1}C_{pm1}+F_{In}C_{pIn}}{M_rC_{pr}+B_wC_{ppol}}(T_{feed}-T^s_{feed})$, we consider the output $y_1 = T - T_s$. This choice yields a relative degree of $r_1 = 1$ with respect to u_1. The input/output dynamics can be then expressed in terms of the time-derivative of the variable: $e_1 = T - T_s$.

2. For the fall-back control configuration with $u_2 = (F_c - F^s_c)a_c$, we choose the output $y_2 = T - T_s$ which yields a relative degree of $r_2 = 2$ and the corresponding variables for describing the input/output dynamics take the form: $e^1_2 = T - T_s$, $e^2_2 = \frac{H_f+H_{g1}-H_{g0}-H_r-H_{pol}}{M_rC_{pr}+B_wC_{ppol}}$. In particular, for the fall-back control configuration, the system describing the input/output dynamics has the following form:

$$\begin{aligned} \dot{e}_2 &= A_2e_2 + l_2(e_2) + b_2\alpha_2u_2 \\ &:= \bar{f}_2(e_2) + \bar{g}_2(e_2)u_2 \end{aligned} \tag{4}$$

where $A_2 = \begin{bmatrix} 0 & 1 \\ 0 & 0 \end{bmatrix}$, $b_2 = \begin{bmatrix} 0 \\ 1 \end{bmatrix}$, $e_2 = \begin{bmatrix} e^1_2 \\ e^2_2 \end{bmatrix}$, $l_2(\cdot) = L^2_{f_2}h_2(x)$, $\alpha_2(\cdot) = L_{g_2}L_{f_2}h_2(x)$, $h_2(x) = y_2$ is the output associated with the fall-back control configuration (the explicit form of the functions $f_2(\cdot)$ and $g_2(\cdot)$ is omitted for brevity). The inverse dynamics, for both the first and second control configurations, have the following form:

$$\begin{aligned} \dot{\eta}_1 &= \Psi_{1,k}(e,\eta) \\ &\vdots \\ \dot{\eta}_{7-r_k} &= \Psi_{7-r_k,k}(e,\eta) \end{aligned} \tag{5}$$

where $k = 1, 2$ and $\Psi_{1,k}\cdots\Psi_{7-r_k,k}$ are nonlinear functions of their arguments describing the evolution of the inverse dynamics of the k-th mode.

Using a quadratic Lyapunov function of the form $V_k = e^T_kP_ke_k$, where P_k is a positive-definite symmetric matrix that satisfies the Riccati inequality $A^T_kP_k + P_kA_k - P_kb_kb^T_kP_k < 0$, we synthesize, for each control-loop, a bounded nonlinear feedback control law (see [15], [7], [8]) of the form:

$$u_k = -r(x, u^{max}_k)L_{\bar{g}_k}V_k \tag{6}$$

where $r(x, u^{max}_k) =$

$$\frac{L^*_{\bar{f}_k}V_k + \sqrt{(L^*_{\bar{f}_k}V_k)^2 + (u^{max}_k|L_{\bar{g}_k}V_k|)^4}}{(|L_{\bar{g}_k}V_k|)^2\left[1+\sqrt{1+(u^{max}_k|L_{\bar{g}_k}V_k|)^2}\right]} \tag{7}$$

and $L^*_{\bar{f}_k}V_k = L_{\bar{f}_k}V_k + \rho|e_k|^2$, $\rho > 0$. The scalar function $r(\cdot)$ in Eqs.6-7 can be considered as a nonlinear controller gain. It can be shown that each controller asymptotically stabilizes the e states in each mode. This result together with the property of the η states can then be used to show, via a small gain argument, for each control configuration, input-to-state stable (we verified this through simulation and analysis of the system of Eq.7 with $e_k = 0$ for both $k = 1$ and $k = 2$). This controller gain, which depends on both the size of actuator constraints, u^{max}_k, and the particular configuration used is shaped in a way that guarantees constraint satisfaction and asymptotic closed-loop stability within a well-characterized region in the state-space. The characterization of this region is discussed in the next step.

(b) *Characterization of constrained stability regions*

Given that actuator constraints place fundamental limitations on the initial conditions that can be used for stabilization, it is important for the control system designer to explicitly characterize these limitations by identifying, for each control configuration, the set of admissible initial conditions starting from where the constrained closed-loop system is asymptotically stable. As discussed in step (c) below, this characterization is necessary for the design of an appropriate switching policy that ensures the fault-tolerance of the control system. The control law designed in step (a) provides such a characterization. Specifically, using a Lyapunov argument, one can show that the set

$$\Theta(u^{max}_k) = \{x \in \mathbb{R}^7 : L^*_{\bar{f}_k}V_k \leq u^{max}_k|L_{\bar{g}_k}V_k|\} \tag{8}$$

describes a region in the state space where the control action satisfies the constraints and the time-derivative of the corresponding Lyapunov function is negative-definite along the trajectories of the closed-loop system. Note that

the size of this set depends, as expected, on the magnitude of the constraints. In particular, the set becomes smaller as the constraints become tighter (smaller u_k^{max}). For a given control configuration, one can use the above inequality to estimate the stability region associated with this configuration. This can be done by constructing the largest invariant subset of Θ, which we denote by $\Omega(u_k^{max})$. Confining the initial conditions within the set $\Omega(u_k^{max})$ ensures that the closed-loop trajectory stays within the region defined by $\Theta(u_k^{max})$, and thereby V_k continues to decay monotonically, for all times that the k-th control configuration is active (see [7] for further discussion on this issue).

An estimate of the region of constrained closed-loop stability for the full system is obtained by defining a composite Lyapunov function of the form $V_{c_k} = V_k + V_{\eta_k}$, where $V_{\eta_k} = \eta^T P_{\eta_k} \eta$ and P_{η_k} is a positive definite matrix and choosing a level set of V_{c_k}, Ω_{c_k}, for which $\dot{V}_{c_k} < 0$ for all x in Ω_{c_k}.

Remark 1: Note that the composite Lyapunov functions, V_{c_k}, used in implementing the switching rules, are in general different from the Lyapunov functions V_k used in designing the controllers. Owing to the ISS property of the η_k-subsystem of each mode, only a Lyapunov function for the e_k subsystem, namely V_k, is needed and used to design a controller that stabilizes the full $e_k - \eta_k$ interconnection for each mode. However, when implementing the switching rules (constructing the Ω_{c_k}), we need to track the evolution of x (and hence the evolution of both e_k and η_k). Therefore, the Lyapunov functions used in verifying the switching conditions at any given time, V_{c_k}, are based on x. From the asymptotic stability of each mode, the existence of these Lyapunov functions is guaranteed by converse Lyapunov theorems.

(c) *Supervisory switching-logic*

Having designed the feedback control laws and characterized the stability region associated with each control configuration, the third step is to derive the switching policy that the supervisor needs to employ to activate/deactivate the appropriate control configurations in the event of faults. The key idea here is that, because of the limitations imposed by constraints on the stability region of each configuration, the supervisor can only activate the control configuration for which the closed-loop state is within the stability region at the time of control system fault. Without loss of generality, let the initial actuator configuration be $k(0) = 1$ and let T_{fault} be the time when this configuration fails, then the switching rule given by

$$k(T_{fault}) \;=\; 2 \;if\; x(T_{fault}) \in \Omega_{c_2}(u_2^{max}) \qquad (9)$$

guarantees asymptotic closed-loop stability. The implementation of the above switching law requires monitoring the closed-loop state trajectory with respect to the stability regions associated with the various actuator configurations. This idea of tieing the switching logic to the stability regions was first proposed in [9] for the control of switched nonlinear systems.

IV. Simulation results

Several simulation runs were carried out to evaluate the effectiveness of the proposed fault-tolerant control strategy. Figure 2 shows the evolution of the open-loop state profiles. Under the operating conditions listed in Table II, the open-loop system behaves in an oscillatory fashion (i.e., the system possesses an open-loop unstable steady-state surrounded by a stable limit cycle). First, process operation

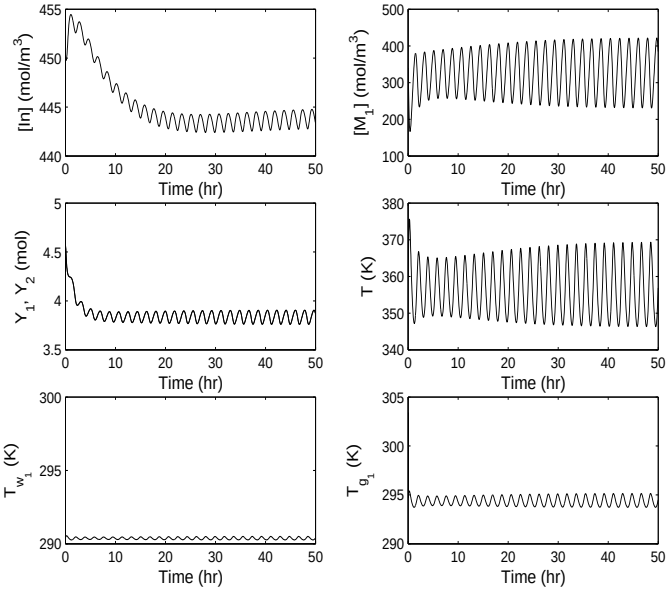

Fig. 2. Evolution of the open-loop state profiles.

under primary control configuration was considered (i.e., the feed temperature, T_{feed}, is the manipulated input) and a bounded nonlinear controller was designed using the formula of Eqs.6-7. Specifically, a quadratic function of the form $V_1 = \frac{1}{2}(T - T_s)^2$ and $\rho_1 = 0.01$ were used to design the controller and a composite Lyapunov function of the form $V_{c_1} = 5\times10^{-3}(In - In_s)^4 + 5\times10^{-4}(M_1 - M_{1s})^2 + 5\times10^{-11}(Y_1 - Y_{1s})^2 + 5\times10^{-11}(Y_2 - Y_{2s})^2 + 5\times10^{-4}(T - T_s)^2 + 5\times10^{-11}(T_{w_1} - T_{w_{1s}})^2 + 5\times10^{-11}(T_{g_1} - T_{g_{1s}})^2$ was used to estimate the stability region of the primary control configuration yielding a $c_1^{max} = 66187.5$. Figure 3 shows the evolution of the closed-loop state profiles and Figure 4 shows the evolution of the manipulated inputs starting from the initial condition $In(0) = 450\ \frac{mol}{m^3}$, $M_1(0) = 340\ \frac{mol}{m^3}$, $Y_1(0) = 4.6\ mol$, $Y_2(0) = 4.6\ mol$, $T(0) = 360\ K$, $T_{w_1}(0) = 300\ K$, and $T_{g_1}(0) = 300\ K$ for which $V_{c_1} = 56.7762$. Since this initial state is within the stability region of the primary control configuration, the controller achieves stabilization of the steady-state.

Next, we consider the case of having a fault in the primary control configuration. In this case, the supervisor has available a fall-back control configuration with the catalyst flowrate, F_c, as the manipulated input. A quadratic Lyapunov function of the form $V_2 = e_2^T P_2 e_2$ and $\rho_2 = 0.01$

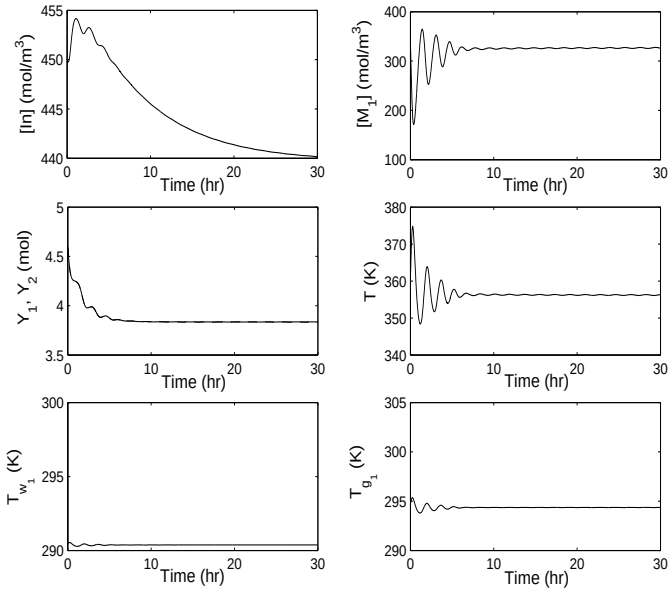

Fig. 3. Closed-loop state profiles under the primary control configuration.

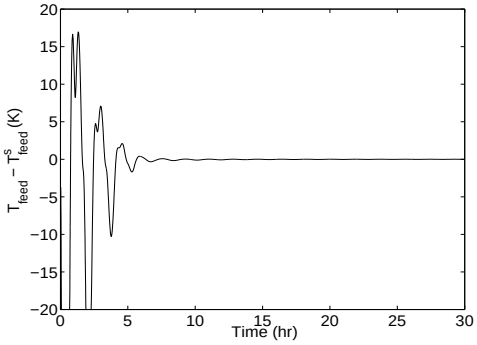

Fig. 4. Manipulated input profile under primary control configuration.

was used to design the controller that uses the fall-back control configuration and a composite Lyapunov function of the form $V_{c_2} = 5 \times 10^{-3}(In - In_s)^4 + 5 \times 10^{-4}(M_1 - M_{1s})^2 + 5 \times 10^{-11}(Y_1 - Y_{1s})^2 + 5 \times 10^{-11}(Y_2 - Y_{2s})^2 + 5 \times 10^{-4}(T - T_s)^2 + 5 \times 10^{-11}(T_{w_1} - T_{w_{1s}})^2 + 5 \times 10^{-11}(T_{g_1} - T_{g_{1s}})^2$ was used to estimate the stability region of the fall-back control configuration yielding a $c_2^{max} = 66187.4$.

To demonstrate that control loop reconfiguration results in fault-tolerant reactor control in the presence of input constraints, we carry out the following simulations: We first initialize the reactor at $In(0) = 450\ \frac{mol}{m^3}$, $M_1(0) = 340\ \frac{mol}{m^3}$, $Y_1(0) = 4.6\ mol$, $Y_2(0) = 4.6\ mol$, $T(0) = 360\ K$, $T_{w_1}(0) = 300\ K$, and $T_{g_1}(0) = 300\ K$ resulting in $V_{c_1} = 56.7762$ which implies that this initial state is within the stability region of the primary control configuration. Consider now, a fault in the primary control configuration at time $T_{fault} = 5.56\ hrs$ (see dashed lines in Figures 5–6). The states of the process at the time of the fault is of the following: $In(T_{fault}) = 449.6575\ \frac{mol}{m^3}$, $M_1(T_{fault}) = 316.9265\ \frac{mol}{m^3}$, $Y_1(T_{fault}) = 3.8573\ mol$, $Y_2(T_{fault}) = 3.8573\ mol$, $T(T_{fault}) = 356.3379\ K$, $T_{w_1}(T_{fault}) = 290.3692\ K$, and $T_{g_1}(T_{fault}) = 294.3422\ K$. In the case of no switching to fall-back control configuration or no backup control configuration available, the system will behave in an oscillatory behavior (solid line in Figure 5). However, applying our fault-tolerant control strategy, the supervisor, then, checks that, if the control configuration were to switched to the fall-back control configuration, $V_{c_2} = 49.5693$, which implies the state at the time of the fault is within the stability region of the fall-back control configuration. Switching to the fall-back control configuration guarantees closed-loop stability (solid lines in Figure 6). Figure 7 shows the manipulated input profiles under primary control configuration (left) and fall-back control configuration (right). Both inputs change smoothly with time to achieve fault-tolerant control.

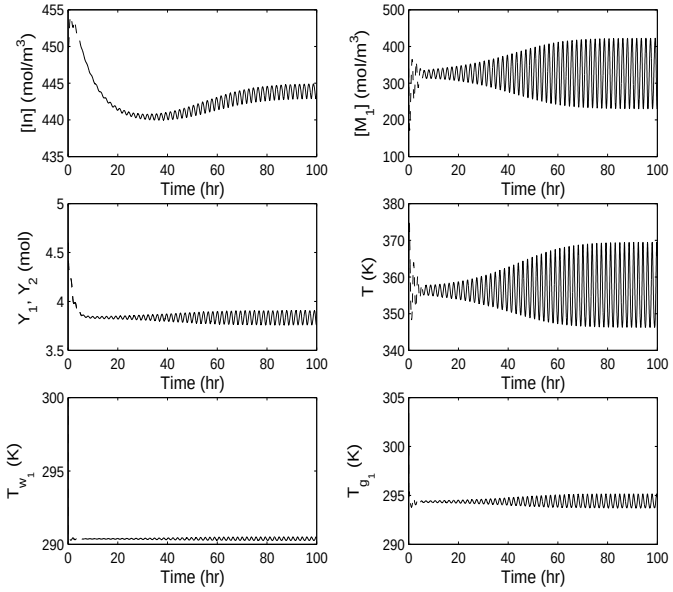

Fig. 5. Evolution of the closed-loop state profiles under primary control configuration (dashed lines) and no fall-back control configuration available to switch to (or fall-back control configuration is not activated) resulting in open-loop oscillatory behavior (solid lines) after primary control configuration fails at $T_{fault} = 5.56\ hrs$.

REFERENCES

[1] J. Bao, W. Z. Zhang, and P. L. Lee. Passivity-based decentralized failure-tolerant control. *Industrial & Engineering Chemistry Research*, 41:5702–5715, 2002.

[2] A. Bemporad and M. Morari. Control of systems integrating logic, dynamics and constraints. *Automatica*, 35:407–427, 1999.

[3] M. Blanke, R. Izadi-Zamanabadi, S. A. Bogh, and C. P. Lunau. Fault-tolerant control systems – a holistic view. *Control Engineering Practice*, 5:693–702, 1997.

[4] K.-Y. Choi and W. H. Ray. The dynamic behavior of fluidized-bed reactors for solid catalyzed gas-phase olefin polymerization. *Chemical Engineering Science*, 40:2261–2279, 1985.

[5] S. A. Dadebo, M. L. Bell, P. J. McLellan, and K. B. McAuley. Temperature control of industrial gas phase polyethylene reactors. *Journal of Process Control*, 7:83–95, 1997.

[6] R. A. Decarlo, M. S. Branicky, S. Petterson, and B. Lennartson. Perspectives and results on the stability and stabilizability of hybrid systems. *Proceedings of the IEEE*, 88:1069–1082, 2000.

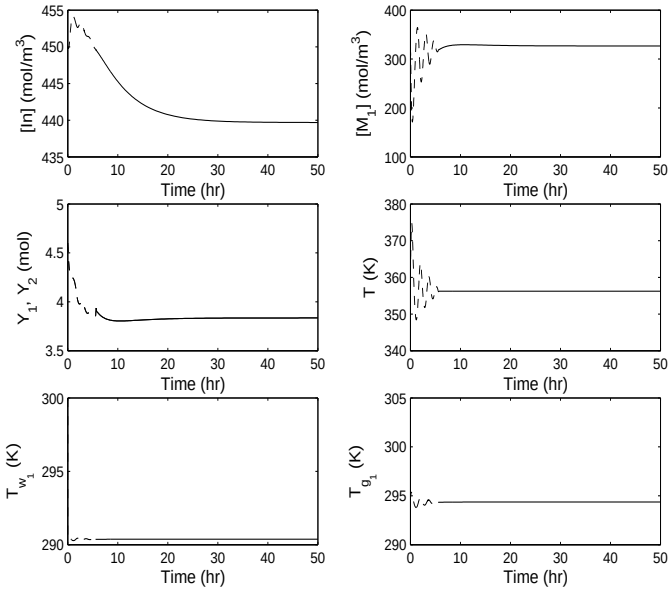

Fig. 6. Evolution of the closed-loop state profiles under primary control configuration (dashed lines) and switching to fall-back control configuration (solid lines) after primary control fails at $T_{fault} = 5.56\ hrs$.

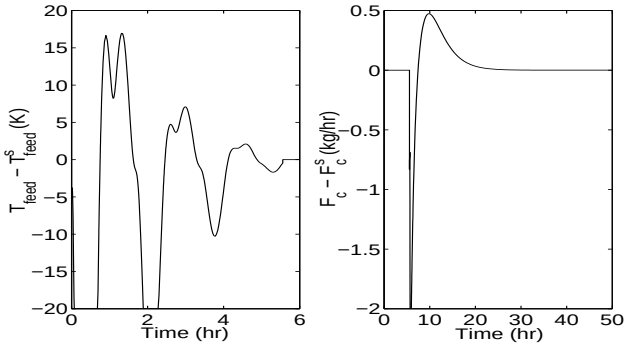

Fig. 7. Manipulated input profiles under primary control configuration (left) fault at $T_{fault} = 5.56\ hrs$ and switching to fall-back control configuration (right).

[7] N. H. El-Farra and P. D. Christofides. Integrating robustness, optimality, and constraints in control of nonlinear processes. *Chemical Engineering Science*, 56:1841–1868, 2001.

[8] N. H. El-Farra and P. D. Christofides. Bounded robust control of constrained multivariabe nonlinear processes. *Chemical Engineering Science*, 58:3025–3047, 2003.

[9] N. H. El-Farra and P. D. Christofides. Coordinated feedback and switching for control of hybrid nonlinear processes. *AIChE Journal*, 49:2079–2098, 2003.

[10] N. H. El-Farra, A. Gani, and P. D. Christofides. Fault-tolerant control of process systems using communication networks. *AIChE Journal*, 51:1665–1682, 2005.

[11] V. Garcia-Onorio and B. E. Ydstie. Distributed, asynchronous and hybrid simulation of process networks using recording controllers. *International Journal of Robust and Nonlinear Control*, 14:227–248, 2004.

[12] I. E. Grossmann, S. A. van den Heever, and I. Harjukoski. Discrete optimization methods and their role in the integration of planning and scheduling. In *Proceedings of 6th International Conference on Chemical Process Control*, pages 124–152, Tucson, AZ, 2001.

[13] K. M. Hangos, J. B. Varga, F. Friedler, and L. T. Fan. Integrated synthesis of a process and its fault-tolerant control-system. *Computers and Chemical Engineering*, 19:S465–S470, 1995.

[14] I. Hyanek, J. Zacca, F. Teymour, and W. H. Ray. Dynamics and stability of polymerization process flow sheets. *Industrial & Engineering Chemistry Research*, 34:3872–3877, 1995.

[15] Y. Lin and E. D. Sontag. A universal formula for stabilization with bounded controls. *Systems & Control Letters*, 16:393–397, 1991.

[16] K. B. McAuley, D. A. Macdonald, and P. J. McLellan. Effects of operating conditions on stability of gas-phase polyethylene reactors. *AIChE Journal*, 41:868–879, 1995.

[17] P. Mhaskar, A. Gani, N. H. El-Farra, P. D. Christofides, and J. F. Davis. Integrated fault-detection and fault-tolerant control for process systems. *AIChE Journal*, submitted.

[18] R. J. Patton. Fault-tolerant control systems: The 1997 situation. In *Proceedings of the IFAC Symposium SAFEPROCESS 1997*, pages 1033–1054, Hull, United Kingdom, 1997.

[19] J. Prakash, S. C. Patwardhan, and S. Narasimhan. A supervisory approach to fault-tolerant control of linear multivariable systems. *Industrial & Engineering Chemistry Research*, 41:2270–2281, 2002.

[20] D. D. Siljak. Reliable control using multiple control systems. *International Journal of Control*, 31:303–329, 1980.

[21] N. E. Wu, K. M. Zhou, and G. Salomon. Control reconfigurability of linear time-invariant systems. *Automatica*, 36:1767–1771, 2000.

[22] T. Y. Xie, K. B. McAuley, J. C. C. Hsu, and D. W. Bacon. Gas-phase ethylene polymerization – production processes, polymer properties, and reactor modeling. *Industrial & Engineering Chemistry Research*, 33:449–479, 1994.

[23] G. H. Yang, S. Y. Zhang, J. Lam, and J. Wang. Reliable control using redundant controllers. *IEEE Transactions on Automatic Control*, 43:1588–1593, 1998.

[24] D. H. Zhou and P. M. Frank. Fault diagnostics and fault tolerant control. *IEEE Transactions on Aerospace and Electronic Systems*, 34:420–427, 1998.